TESTING WITH REAL DATA A WEIGHTED LEAST-SQUARES METHOD FOR PSI

Fernando Vicente-Guijalba and Juan M. Lopez-Sanchez

Signals, Systems and Telecommunications Group, University of Alicante, P.O. Box 99, E-03080 Alicante, Spain

ABSTRACT

This paper presents an analysis of the performance with real data of a recently proposed PSI approach based on Least Squares. based PSI approach for urban subsidence monitoring using TerraSAR-X and ERS-1/2 data. For this purpose, two different test sites and data sets have been selected. On the one hand, the city of Murcia (Spain), affected by large areas of subsidence due to groundwater exploitation, has been studied with TerraSAR-X images. On the other hand, the city of Alcoy (Spain) is affected by deformation only over small areas. In the second case, a set of ERS-1/2 images is used for evaluating the algorithm.

1. INTRODUCTION

Persistent Scatterer Interferometry (PSI) allows us to detect and monitor ground subsidence phenomenon. PSI classical approaches need phase unwrapping in some part of the processing. The original PS approach, as shown in [1], overcomes phase unwrapping through an integration step, remarking that no ambiguity should exist between nodes to correctly estimate linear components. The SBAS approach, exposed in [2], works with an stack of interferograms which have been previously unwrapped. Despite many unwrapping techniques have been developed and applied for using multitemporal data, one can still find some scenarios where these techniques yield wrong results due to the presence of aliasing, multipath inconsistencies and noise.

Recently a new PSI approach which avoids phase unwrapping was introduced in [3]. This approach employs a Weighted Least Squares (WLS) adjustment in order to estimate the linear component increments between two PS's: $\Delta\varepsilon_{DEM}$ and Δv. An outlier detector for the links between PS's is defined and exploited, so estimates exceeding the threshold are eliminated from the solution. Finally, an integration step with all survivor links is carried out to obtain a linear deformation rate map and a DEM error map. However, all results presented in [3] were obtained with simulated data. Therefore, the first objective of this work is to test this algorithm with real satellite data. In addition, an alternative way to obtain the weights used in the WLS approach is introduced.

2. THEORETICAL FRAMEWORK

The three main characteristics introduced in [3] to overcome phase unwrapping in PSI are, namely: the use of an alternative Delaunay triangulation network, the a priori characterization of the link quality, with a convenient parameter, and the estimation procedure using a Weighted Least Square methodology. We revisit here these main topics to understand how this technique avoids phase unwrapping and allows us to estimate linear deformation rates and DEM errors.

2.1. Local triangulation network

In this approach, as in many others, the relative linear terms between PS have to be estimated. A Delaunay triangulation of the set of PS is usually performed to get a set of links over the whole scene. Although some distance restrictions must be done after triangulation (usually links longer than 1 km are removed), this triangulation does not provide the optimal shortest link network, and, more importantly, does not provide any redundance in the way the PS are linked. In the proposed approach, however, a Delaunay triangulation is applied over small patches around each PS. For each point all PS inside a buffer of $300 - 400$ m are taken into account to perform the local triangulation. As illustrated in Figure 1, this is repeated for each PS, but considering only once those overlapped links. This procedure creates a redundant network with optimal shortest arcs.

2.2. Link estimator quality

The authors of [3] propose an a priori Variance Components estimation of the double-differences phases, using the variance-covariance matrix of the random noises for each image. This a priori quality estimator enables a LS computation of the linear estimation taking into account the phase data quality. This approach works fine with simulated data, but we are unable to determine how to compute the VC matrix from real satellite images. Instead, we propose in this work a feasible alternative.

Our approach is based on the known relationship between the phase standard deviation and the estimated coherence

Proc. 'Fringe 2011 Workshop', Frascati, Italy,
19–23 September 2011 (ESA SP-697, January 2012)

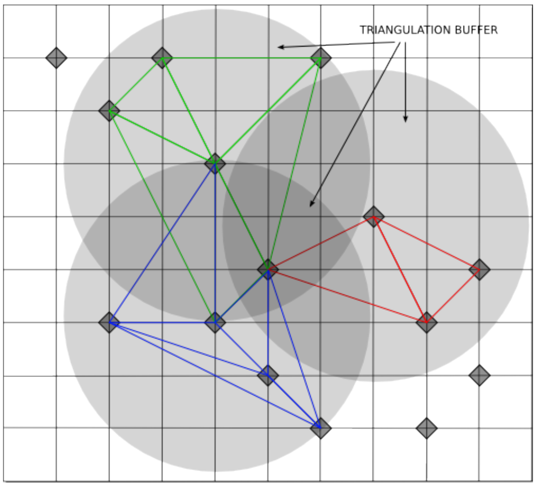

Figure 1. Local Delaunay Triangulation around each PS. Overlapped links are only considered once.

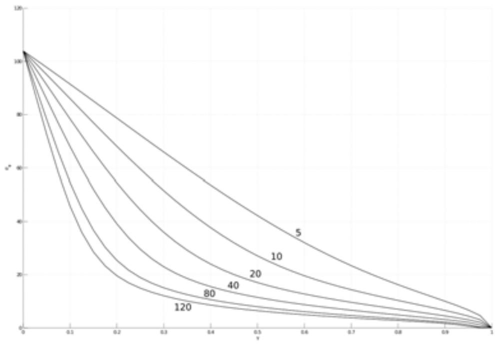

Figure 2. Phase standard deviation (σ_ϕ) as a function of coherence (γ) and effective number of looks (ENL).

and effective number of looks, through the Probability Density Function for InSAR data (Figure 2).

Once $\sigma^k_{\phi,m}$ is obtained for each PS and each interferogram in the stack, as shown in Figure 3, it is possible to determine an estimation of the standard deviation of the link using expression (1). Note that we are always considering multi-looked interferograms. For each link composing the network it is possible to create a VC matrix as in expression (2). This matrix is used next as a measure of the quality of the link in the stack.

$$\sigma_{mn} = \sqrt{\sigma_m^2 + \sigma_n^2} \tag{1}$$

$$P^{dd} = Q_{dd}^{-1} = \begin{bmatrix} 1/\sigma^2_{1,mn} & 0 & \cdots & 0 \\ 0 & 1/\sigma^2_{2,mn} & \cdots & 0 \\ \vdots & \vdots & \ddots & \vdots \\ 0 & 0 & \cdots & 1/\sigma^2_{k,mn} \end{bmatrix} \tag{2}$$

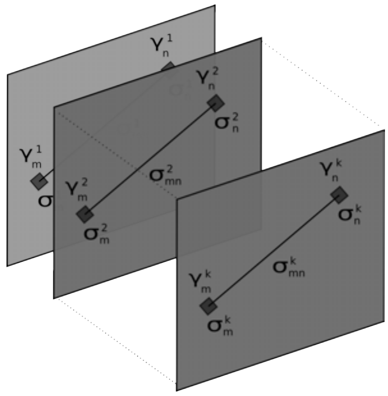

Figure 3. The phase standard deviation of a link for each interferogram is obtained using the estimations of phase standard deviation of each node.

2.3. Weighted Least-Squares Estimator

The differential phase in the link between PS (nodes) m and n, at interferogram k, is composed by a set of terms as shown in expression (3). The first two terms are related with the incremental error relative to the extracted synthetic DEM ($\Delta\varepsilon_{DEM,mn}$ and the linear deformation variation (Δv_{mn}) between both nodes. The remaining terms are related to the non linear deformation phenomenon, atmospheric artifacts between acquisitions, Doppler centroid variations and noise.

$$\begin{aligned} \Delta\phi^k_{mn} &= \Delta\phi^k(x_m, y_m) - \Delta\phi^k(x_n, y_n) \\ &= \frac{4\pi}{\lambda} \cdot \frac{B^k_n}{r_0 \cdot \sin\alpha} \cdot \Delta\varepsilon_{DEM,mn} + \frac{4\pi}{\lambda} \cdot \Delta v_{mn} \cdot B^k_t \\ &+ \Delta\rho^k_{nonlin,mn} + \Delta\phi^k_{atm,mn} + \Delta\phi^k_{fdc,mn} + \Delta\phi^k_{noise,mn} \end{aligned} \tag{3}$$

For simplification, it is possible to express this phase model as in (4).

$$\begin{aligned} \Delta\phi^k_{mn} &= \alpha^k_{mn}\Delta\varepsilon_{mn} + \beta^k\Delta v_{mn} + w^k_{mn} \\ w^k_{mn} &= \Delta\rho^k_{nonlin,mn} + \Delta\phi^k_{atm,mn} + \Delta\phi^k_{fdc,mn} + \Delta\phi^k_{noise,mn} \end{aligned} \tag{4}$$

Thus, the problem of estimating the linear components for each link can be addressed as the solution of the equation system shown in (5).

$$\begin{aligned} \Delta\Phi &= A \cdot \begin{bmatrix} \Delta\varepsilon_{DEM,mn} \\ \Delta v_{mn} \end{bmatrix} + W \\ \Delta\Phi &= \begin{bmatrix} \Delta\phi^1_{mn} & \Delta\phi^2_{mn} & \cdots & \Delta\phi^k_{mn} \end{bmatrix}^T \\ A &= \begin{bmatrix} \alpha^1_{mn} & \alpha^2_{mn} & \cdots & \alpha^k_{mn} \\ \beta^1_{mn} & \beta^2_{mn} & \cdots & \beta^k_{mn} \end{bmatrix}^T \\ W &= \begin{bmatrix} w^1_{mn} & w^2_{mn} & \cdots & w^k_{mn} \end{bmatrix} \end{aligned} \tag{5}$$

Considering that no phase ambiguity is present in the set of observables, $\Delta\Phi$, it is possible through LS to obtain an estimation of the two linear terms, $\Delta\hat{\varepsilon}_{DEM,mn}$ and $\Delta\hat{v}_{mn}$, as expressed in (6). The differences between the real set of observables and the modeled ones is known as residues, r.

$$\begin{aligned} \begin{bmatrix} \Delta\hat{\varepsilon}_{DEM,mn} \\ \Delta\hat{v}_{mn} \end{bmatrix} &= (A^T P^{dd} A)^{-1} A^T P^{dd} \Delta\Phi \\ \Delta\hat{\Phi} &= A(A^T P^{dd} A)^{-1} A P^{dd} \Delta\Phi \\ r &= \Delta\Phi - \Delta\hat{\Phi} \end{aligned} \tag{6}$$

In the same LS context, it is also possible to obtain some quality parameters from the estimated results. The VC matrices of the estimated quantities are expressed in (7).

$$\begin{aligned} D\left\{\begin{bmatrix} \Delta\hat{\varepsilon}_{DEM,mn} \\ \Delta\hat{v}_{mn} \end{bmatrix}\right\} &= Q_{\hat{x}\hat{x}} = (A^T P^{dd} A)^{-1} \\ D\{\Delta\hat{\Phi}\} &= Q_{\Delta\hat{\Phi}\Delta\hat{\Phi}} = A(A^T P^{dd} A)^{-1} A^T \\ D\{r\} &= Q_{vv} = Q_{dd} - A(A^T P^{dd} A)^{-1} A^T \end{aligned} \tag{7}$$

Those arcs with potential phase ambiguities are detected by applying an outlier detector and then removed from the final solution. Since link differential phases with phase ambiguities tend to increase the corresponding residual, a simple outlier detector consists in the evaluation of the maximum residual value as expressed in (8). If that value is above a predefined threshold, then the link is considered as an outlier and removed from the solution. Otherwise, it is maintained in the processing.

$$Max(|r_i|) > c\sqrt{(Max(Q^{dd})_{ii})} + 2\sqrt{(Max(Q_{\Delta\hat{\Phi}\Delta\hat{\Phi}})_{ii})} \tag{8}$$

Finally, as in other conventional PSI approaches, in this WLS–PSI technique it is necessary to perform an integration step to obtain deformation rate and DEM error values at pixel level.

3. TEST OVER REAL SCENARIOS

Several results with simulated input data were presented in [3]. In this work we present results obtained over two real scenarios. The first one using TerraSAR-X images. The second one has been done using ERS-1/2 images.

3.1. Murcia Study With TerraSAR-X Data

Subsidence phenomenon has occurred in the metropolitan area of Murcia city (SE Spain) as a result of soil consolidation due to piezometric level depletion caused by

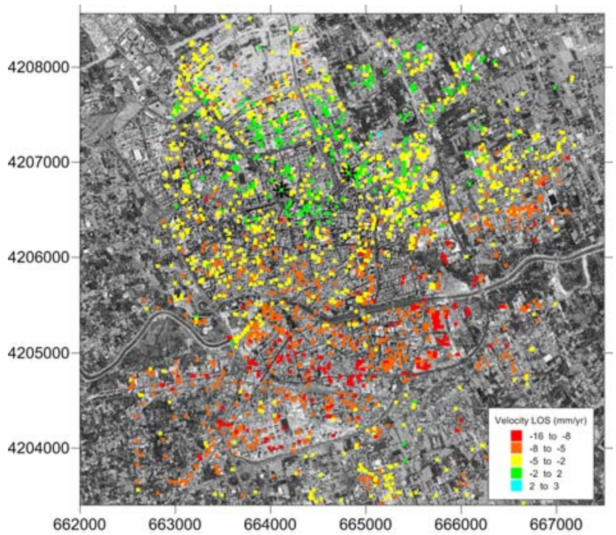

Figure 4. Linear deformation rate map obtained in Murcia (2008–11). Negative velocity stands for movements away from sensor.

excessive pumping of groundwater [4]. As a first case study, we want to determine how the WLS–PSI approach behaves in this scenario.

Results have been obtained with a stack of 72 TerraSAR-X single-pol VV images acquired over 3 years, from July 18th 2008 to August 19th 2011. From the data set, 192 differential interferograms have been generated with spatial baselines below 160 m, temporal baselines below 200 days, and Doppler increments below 500 Hz. A multilook of 15×15 pixels (range $\times$ azimuth) has been used, and the coherence threshold for accepting or rejecting a multilooked pixel as a PS has been set to 0.70 at 50% (min. 0.01).

The obtained LOS velocity map for this scenario is shown in Figure 4. As expected from previous studies [4], the north part of the city of Murcia is quite stable, wheras the south part exhibits high subsidence values over large areas. Points reaching up to -16.0 mm/year are detected in this area.

3.2. Alcoy Study With ERS-1/2 Data

From our previous experience with other conventional PSI approaches, they fail to measure correct subsidence values in the area of Alcoy city (SE Spain). In this work, we tested the WLS–PSI approach in this scenario. Results have been obtained with a stack of 25 ERS-1/2 images acquired from April 23th 1995 to December 18th 2000. From that data set, 48 differential interferograms have been generated with spatial baselines below 300 m, temporal baselines below 1000 days and Doppler increments below 500 Hz. A multilook of 4×20 (range $\times$ azimuth) has been used, and the coherence threshold for accepting or rejecting a multilooked pixel as a PS has been

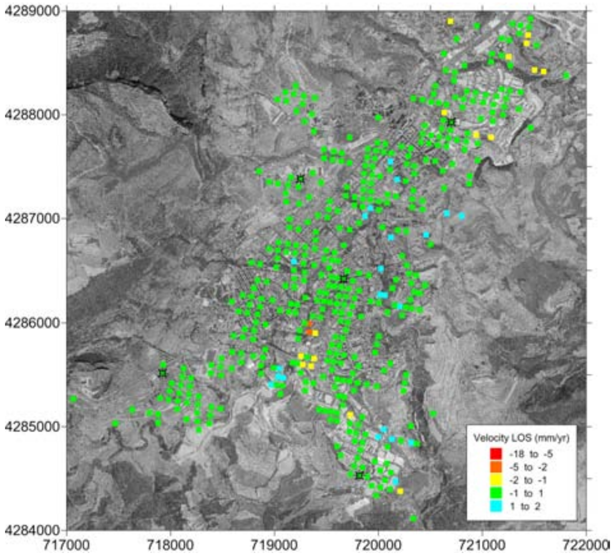

Figure 5. Linear deformation rate map obtained in Alcoy (1995–2000). Negative velocity stands for movements away from sensor.

set to 0.40 at 40% (min. 0.01).

The LOS velocity map obtained in this case is shown in Figure5. Some small deformation areas are spotted at the central part of the city, but higher velocity rates were expected. Therefore, deformation rates have been underestimated in this case.

4. CONCLUSIONS

It has been proven that the WLS–PSI approach proposed in [3] works correctly in areas with high density of stable points, i.e. providing a network with short arcs, and with smooth spatial variations. In such conditions, this algorithm provides results similar to those obtained with previous PSI algorithms.

On the other hand, in scenarios where small localized areas with significant deformation are expected, the WLS–PSI technique yields an underestimation of the linear velocity solution. The proposed adjustment model only works for linear link solutions and, consequently, those links with phase ambiguities which are not correctly discarded with the proposed outlier detector produce an underestimated solution. Accordingly, future work should be addressed to provide a more reliable outlier detector to overcome this situation.

ACKNOWLEDGMENTS

TerraSAR-X images have been provided by DLR in the framework of project GEO0389 of the TerraSAR-X scientific program. ERS-1/2 images have been provided by ESA in the framework of project Cat 1. 3148. This work has been supported by the Spanish Ministry of Science and Innovation (MICINN) under Project TEC2008-06764-C02-02.

REFERENCES

[1] Ferretti, A., Prati C. & Rocca F. (2000). Nonlinear Subsidence Rate Estimation Using Permanent Scatterers in Differential SAR Interferometry. *IEEE Trans. Geosci. Remote Sensing*. **38**(5), 2202-2212.

[2] Berardino, P., Fornaro, G., Lanari, R. & Sansosti, E. (2002). A new algorithm for surface deformation monitoring based on small baseline differential SAR interferograms. *IEEE Trans. Geosci. Remote Sensing*. **40**(11), 2375-2383.

[3] Zhang, L., Ding, X. & Lu, Z. (2011). Modeling PSInSAR Time Series Without Phase Unwrapping. *IEEE Trans. Geosci. Remote Sensing*. **49**(1), 547-556.

[4] Herrera, G. et. al. (2010). Analysis of subsidence using TerraSAR-X data: Murcia case study. *Engineering Geology*. **116**(3-4), 284-295.